# THERMAL-BARRIER MULTILAYER PLASMA COATINGS $ZrO_2$–NiCrAlY

**A.L. BORISOVA, A.Yu. TUNIK, L.I. ADEEVA, A.V. GRISHCHENKO, T.V. TSYMBALISTAYA** and **M.V. KOLOMYTSEV**
E.O. Paton Electric Welding Institute, NASU, Kiev, Ukraine

Comparative characteristics of multilayer plasma coatings $ZrO_2$–NiCrAlY are given. It is established that phase composition of the external ceramic layer depends on thickness of the metallic interlayer, i.e. its thermal conductivity that affects the rate of cooling of the $ZrO_2$ particles deposited on it. Thickness of the metallic interlayer should not exceed 100 μm to ensure optimal heat resistance of the ceramic layer.

***Keywords:*** *zirconia, alloy NiCrAlY, powders, plasma spraying, multilayer coatings, phase composition, structure, heat resistance of coatings*

Many pressing problems of modern engineering, one of the most important among which is improving the efficiency and quality of power machines, can be successfully solved by applying thermal barrier coatings (TBC). The world-wide experience of using TBCs on parts of internal combustion engines allows optimising working conditions of the engines, increasing their efficiency, reducing consumption of fuel and lubricants, decreasing toxicity of exhaust gases, etc. Plasma coatings with an external ceramic layer of partially stabilised zirconia and metallic interlayer of NiCrAlY are recognised to be the most suitable TBCs for internal combustion engines [1]. Heat resistance and service life of coatings based on $ZrO_2$, which is characterised by polymorphic transformations and substantial volume changes taking place in heating and cooling, depend to a considerable degree upon the phase composition of the thermal barrier layer formed during spraying.

The optimal phase composition of the external ceramic layer is considered to be the maximal content of the so-called tetragonal T′-phase with a low degree of tetragonality, providing high heat resistance, as well as the presence of an insignificant (4–5 wt.%) content of the monoclinic phase. Martensitic transformation of the latter leads to formation of a network of fine cracks in the coating, thus preventing its fracture [2–5]. The T′-phase is structurally identical to the tetragonal T-phase, but it differs in an increased content of $Y_2O_3$ dissolved in it, this leading to growth of the volume of a tetragonal phase cell and simultaneous decrease of the degree of tetragonality down to one, i.e. to transformation into a structure of cubic modification.

Many issues related to formation of the optimal phase composition of the external ceramic layer of TBC (chemical composition and fraction of a spraying powder, technological parameters of the spraying process, coating thickness, etc.) are studied in sufficient detail. However, this process can also be affected by such unstudied factors as conditions of cooling of particles of the sprayed ceramic layer, including those that also depend upon the thickness of the metallic interlayer.

One of the ways of improving heat resistance of TBC is to form graded coatings, the composition of which gradually changes from the metallic interlayer to the external ceramic layer [6–8]. It is thought that transition cermet layers deteriorate thermal fatigue properties of the coatings at a temperature above 1170–1220 K, which is caused by intensive oxidation of the metallic component of a transition layer [3]. This leads to initiation of extra compressive stresses within the coating and premature exfoliation of the ceramic layer.

The purpose of this study was to address two problems: investigation of the effect of thickness of the metallic NiCrAlY layer on phase composition of the external ceramic $ZrO_2$ layer to determine its optimal value, and evaluation of peculiarities of formation and structure of multilayer coatings $ZrO_2$–NiCrAlY, involving comparative tests of aluminium parts of internal combustion engines with such coatings to heat resistance under thermal cycling conditions.

The $ZrO_2$ powder stabilised by 6.2 wt.% $Y_2O_3$ was used as a material for deposition of the external ceramic layer of TBC, and the NiCrAlY powder of alloy PKh16N77Yu6I produced by the calcium reduction method was used as a material of the metallic interlayer. Its chemical composition was as follows, wt.%: 73.64–75.44 Ni, 17.02–17.58 Cr, 5.78–5.86 Al, 0.88–1.07 Y, and 0.87–1.85 Ca.

Mixtures of the powders for deposition of multilayer coatings were prepared in air in the laboratory attritor at a minimal rotation speed of the impeller equal to 400 rpm for 30 min. The powder mixtures had the following chemical composition: $(100 - n)$NiCrAlY + $n ZrO_2$, where $n$ = 0, 50 and 100 (for three-layer coatings), or 0, 25, 50, 75 and 100 wt.% (for five-layer coatings).

The plasma coatings were deposited by using machine UPU-8M. Steel samples were used as a coating

**Table 1.** Spraying parameters for plasma coatings*

| Composition of spraying powder, wt.% | Fraction, μm | *U*, V | Plasma gas | | Spraying distance, mm |
|---|---|---|---|---|---|
| | | | Composition | Flow rate, l/min | |
| NiCrAlY | −100 − +40 | 40 | Ar + $N_2$ | 24 | 130 |
| 25$ZrO_2$ + 75NiCrAlY | −60 − +40 | 40 | Ar + $N_2$ | 26 | 130 |
| 50$ZrO_2$ + 50NiCrAlY | | 50 | Ar + $N_2$ | 28 | 120 |
| 75$ZrO_2$ + 25NiCrAlY | | 55 | $N_2$ | 30 | 120 |
| $ZrO_2$ | | 60 | $N_2$ | 31 | 100 |

*Spraying current $I$ = 500 A.

substrate, and aluminium alloy samples were used to study heat-protecting properties. The deposition parameters were adjusted depending on the composition of a spraying material (Table 1).

Investigation of the powders and coatings was carried out by metallography using microscope «Neophot-32» with an attachment for digital photography, scanning electron microscopy (electron microscope JSM-840), durometric analysis (LECO hardness meter M-400 under a load of 0.25 N), and X-ray diffraction phase analysis (diffractometer DRON-UM1, Cu$K_\alpha$ radiation). Data of the diffractometry experiment were processed by using software PowerCell 2.4 for full-profile analysis of X-ray spectra of a mixture of polycrystalline phase components.

Heat-protective properties of the coatings were investigated by subjecting their surfaces to direct heating with a gas torch jet flame, and the $C_3H_8$ + $O_2$ gas mixture with a volume ratio of 1:3 was used as a fuel mixture. The torch was placed at a distance of 35–40 mm from the surface of a coated sample. The samples were heated for 3 s to a temperature of 400 °C and cooled with air flow approximately for 20 s, and then with water approximately for 6 s to a temperature of 70–80 °C. The temperature of the samples was determined by using digital multimeter UT-70B. Thermal cycling was carried out up to violation of integrity of a coating or its separation from the substrate to no more than 15 %.

**Characteristics of initial powders.** The $ZrO_2$ powder stabilised with 6.2 wt.% $Y_2O_3$ (Figure 1, *a, b*) consisted of particles of an irregular fragmented shape with sharp edges, 40–60 μm in size. According to the results of X-ray diffraction phase analysis, it contained 89.8 wt.% of the tetragonal phase (T-$ZrO_2$) and 10.2 wt.% of the monoclinic (M-$ZrO_2$) phase (Figure 1, *c*).

The powder of alloy NiCrAlY consisted of irregular particles in the form of conglomerates with a size of 40–100 μm (Figure 1, *d, e*). According to the data of X-ray diffraction phase analysis, it contained the following phases: γ-nickel solid solution and γ′-$Ni_3Al$ in-

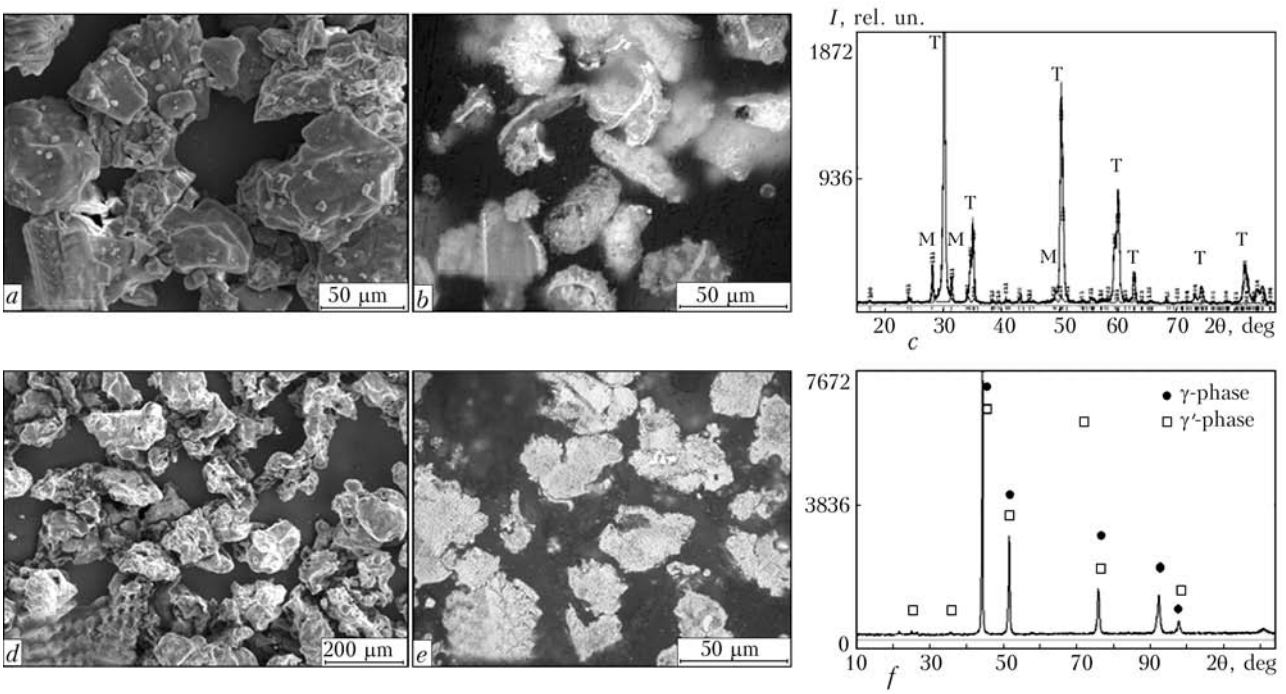


**Figure 1.** Appearance (*a, d*), microstructure (*b, e*) and X-ray patterns (*c, f*) of powders $ZrO_2$ + 6.2 wt.% $Y_2O_3$ (*a–c*) and NiCrAlY (*d–f*)

'**Table 2.** Characteristics of two-layer $ZrO_2$–NiCrAlY coatings with different thickness of metallic interlayer

| Thickness of metallic interlayer, μm | | Phase composition of ceramic layer | *HV*, MPa | |
|---|---|---|---|---|
| NiCrAlY | $ZrO_2$ | | NiCrAlY | $ZrO_2$ |
| ~50 | 200–230 | T-$ZrO_2$, traces of M-$ZrO_2$ | 2630 ± 540 | 11,990 ± 1420 |
| ~100 | 200–250 | T-$ZrO_2$, traces of M-$ZrO_2$ | 3110 ± 560 | 11,230 ± 2130 |
| ~150 | 200–210 | T-$ZrO_2$, C-$ZrO_2$ (12 wt.%), traces of M-$ZrO_2$ | 3130 ± 500 | 11,020 ± 1110 |

*Note*. C — cubic modification of $ZrO_2$.

termetallic (Figure 1, *f*). Structure of the particles was a nickel-based solid solution (γ-phase) reinforced with dispersed particles of $Ni_3Al$ (γ′-phase).

**Two-layer plasma coatings.** Investigation of the effect of thickness of the NiCrAlY interlayer on phase composition and properties of the ceramic layer of TBC showed that thickness of the ceramic layer was approximately identical in all the samples and equal to about 200 μm, while thickness of the metallic interlayer varied from 50 to 150 μm. Characteristics of the two-layer $ZrO_2$–NiCrAlY coatings are given in Table 2.

It was found that in all the cases the formed two-layer coating was dense, having no cracks and delaminations at both interfaces between the ceramics and interlayer and between the binding layer and substrate (Figure 2). The metallic interlayer had a clearly defined lamellar structure with thin oxide intermediate layers along the lamellar boundaries. Microhardness of the interlayer grew from 2630 to 3130 MPa with

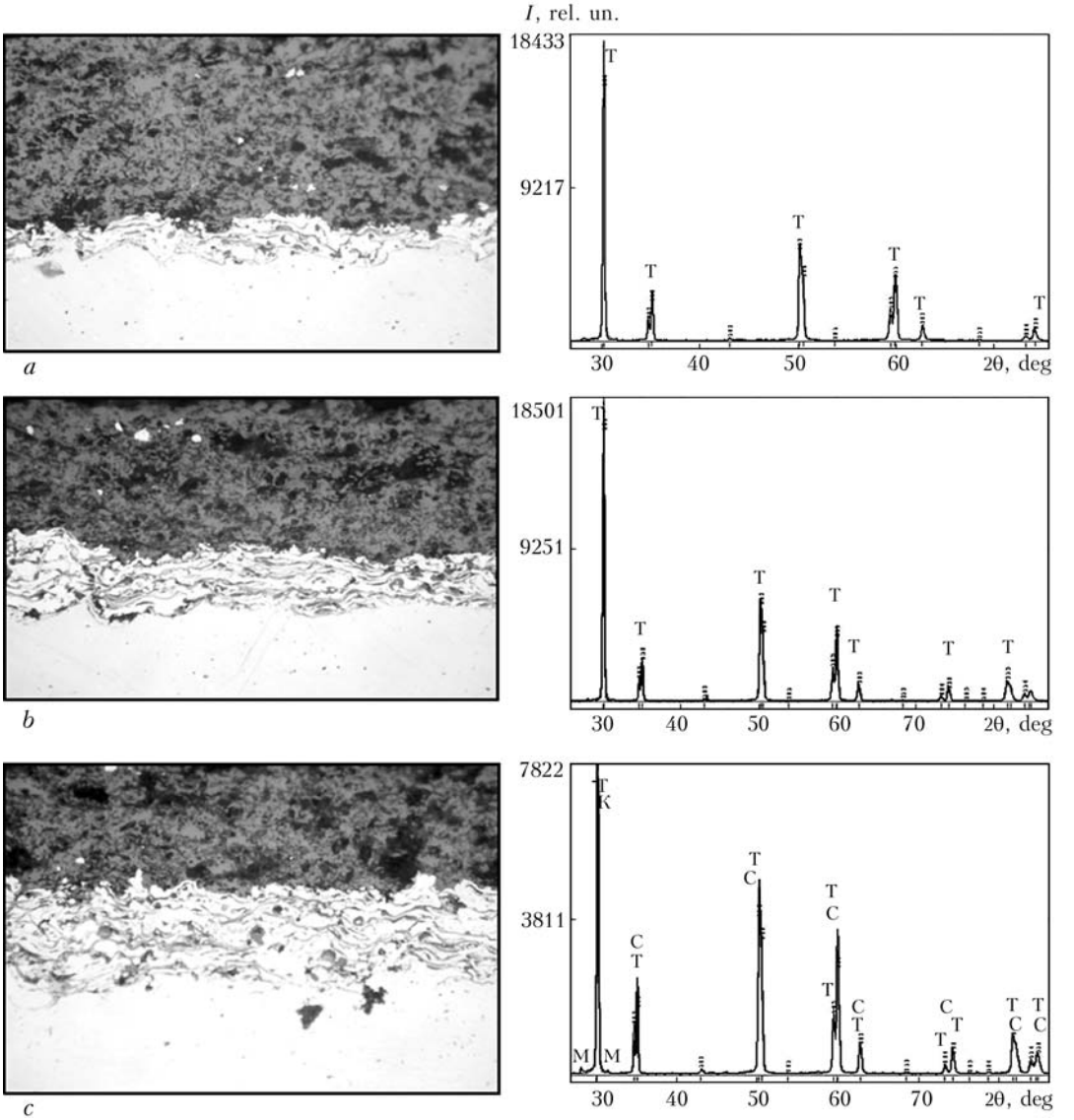


**Figure 2.** Microstructure (×200) (*left*) and X-ray patterns (*right*) of two-layer plasma coatings with metallic interlayer 50 (*a*), 100 (*b*) and 150 (*c*) μm thick

**Table 3.** Effect of thickness of metallic interlayer on phase composition and crystalline lattice parameters (*a, c, b*) of phases of $ZrO_2$ ceramic layer

| Investigation object | Thickness of NiCrAlY interlayer, μm | Phase composition of ceramic layer | | | | | | | |
|---|---|---|---|---|---|---|---|---|---|
| | | T-$ZrO_2$ | | | | M-$ZrO_2$ | | | |
| | | *a*, nm | *c*, nm | *c*/*a* | $V \cdot 10^3$, $nm^3$ | *a*, nm | *b*, nm | *c*, nm | β, deg |
| Powder $ZrO_2$ | – | 0.51047 | 0.51672 | 1.0122 | 134.6469 | 0.51439 | 0.52081 | 0.53230 | 99.16 |
| Powder $ZrO_2$* | 50 | 0.51078 | 0.51623 | 1.0107 | 134.6823 | 0.51460 | 0.52120 | 0.53130 | 99.20 |
| | 100 | 0.51079 | 0.51629 | 1.0108 | 134.7030 | 0.51668 | 0.52044 | 0.53237 | 99.20 |
| | 150 | 0.51054 | 0.51632 | 1.0113 | 134.5793 | 0.51713 | 0.52714 | 0.52771 | 99.20 |

*$a$ = 0.51147 nm for C-$ZrO_2$ modification.

increase in its thickness (see Table 2). According to the data of X-ray diffraction phase analysis, phase composition of the interlayer was as follows: nickel-based solid solution, γ′-$Ni_3Al$, β-NiAl, and solid solution of nickel in chromium α-Cr. Unlike the composition of the spraying powder, new phases β-NiAl, NiO and α-Cr appeared in the coating, which formed as a result of flowing of the particles through the plasma jet.

The ceramic layer of all the coatings had no lamellar structure, and microhardness of the coatings was approximately the same (about *HV* 11,000 MPa). Thickness of the metallic interlayer had almost no effect on structure and microhardness of the $ZrO_2$ layer. However, it changed its phase composition. With a coating deposited on the metallic interlayer 50 and 100 μm thick, the main phase of the ceramic layer was the tetragonal phase, while the weight content of the monoclinic phase decreased to 2 % compared with the initial powder, where its content was 10.2 wt.%. In the case of the 150 μm thick interlayer, the ceramic layer also contained about 12 wt.% of cubic modification of $ZrO_2$, in addition to the above phases (see Figure 2). At a depth of 100 μm from the surface, phase composition of the ceramic layer of all the coatings was practically identical. It was a mixture of the tetragonal phase with 4 wt.% of the monoclinic phase.

Evaluation of the degree of tetragonality and volume of an elementary cell of the tetragonal $ZrO_2$ phase showed that at an interlayer thickness of 150 μm the degree of tetragonality of $ZrO_2$, *c*/*a*, was 1.0113, and volume of the elementary cell was $V = 134.5793 \cdot 10^{-3}$ $nm^3$. At an interlayer thickness of 50 and 100 μm, the phase formed had a lower degree of tetragonality (*c*/*a* = = 1.0107 and 1.0108) and an increased volume of the elementary cell, $V = 134.6823 \cdot 10^{-3}$ and $134.7030 \cdot 10^{-3}$ $nm^3$, respectively (Table 3). These phases are close in their structure to the T′-$ZrO_2$ quench phase, which, according to literature data [9], is characterised by resistance to both low and high temperatures, and by an increased stability at cyclic temperature changes. Therefore, the preferable thickness of the NiCrAlY interlayer is no more than 100 μm.

**Multilayer coatings.** Spraying of multilayer coatings was preceded by making and investigation of samples with one-layer coatings of powder mixtures with 25, 50 and 75 wt.% $ZrO_2$.

It was found that all the coatings of the powder mixtures were uniform in thickness, had no cracks, and tightly adhered to the substrate (Figure 3). Increasing the NiCrAlY content of the spraying powder was accompanied by growth of the quantity of metallic particles with a round or lamellar shape in the structure. The coating with a minimal content of the ceramic component (25 wt.%) was characterised by the highest lamellar content (see Figure 3, *c*). Microhardness of the coatings dramatically grew with increase of the zirconia content of the layer: *HV* 4760 ± 1810, 5150 ± 1190 and 7310 ± 2250 MPa at 25, 50 and 75 wt.% $ZrO_2$ (Table 4). According to the data of X-ray diffraction phase analysis, the composition of the cermet layers was almost constant and included different combinations of phases: γ-nickel-based solid solution, γ′-$Ni_3Al$, T-$ZrO_2$, M-$ZrO_2$, NiO and α-Cr

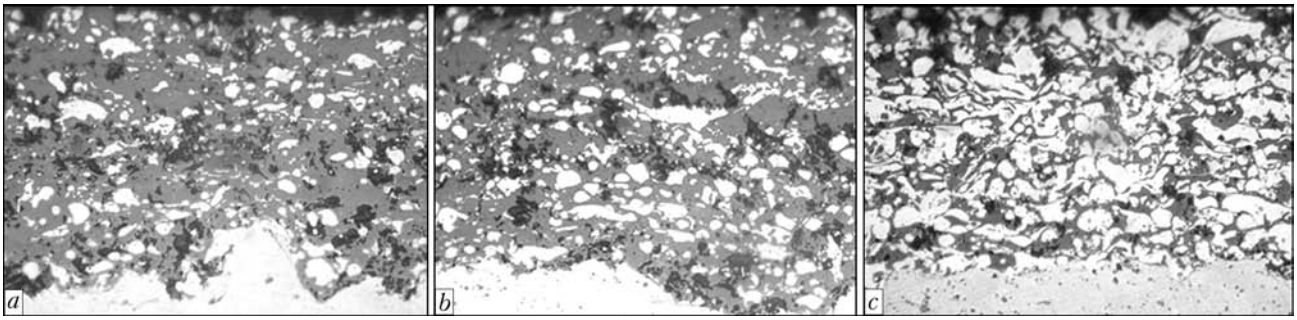


**Figure 3.** Microstructure (×400) of plasma coatings produced from different powder mixtures, wt.%: *a* — $75ZrO_2$ + 25NiCrAlY; *b* — $50ZrO_2$ + 50NiCrAlY; *c* — $25ZrO_2$ + 75NiCrAlY

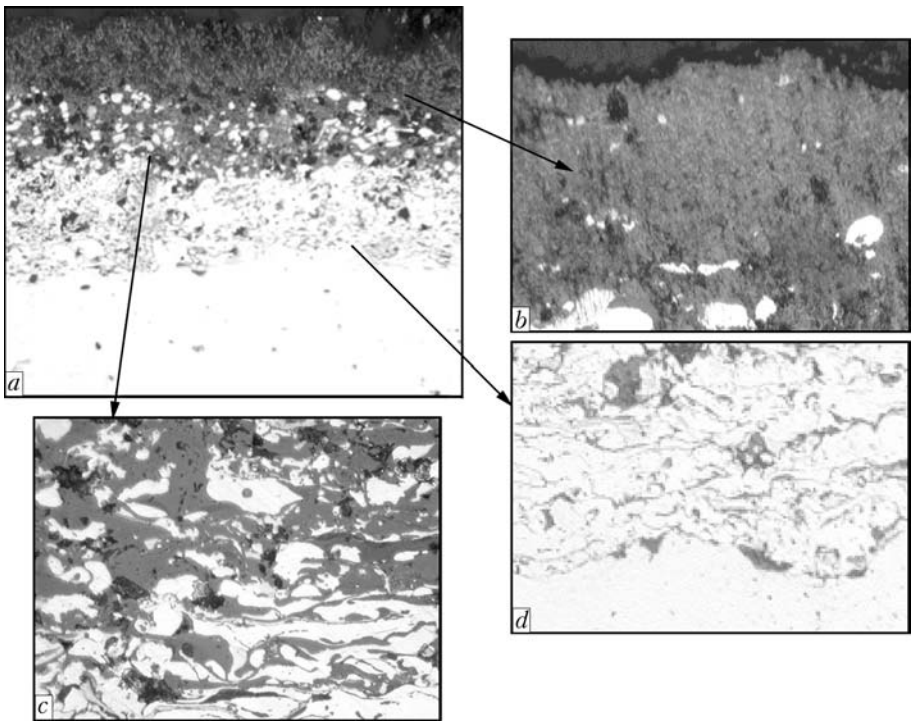


**Figure 4.** Microstructure of three-layer plasma coating: *a* — general view (×200); *b* — external $ZrO_2$ layer; *c* — intermediate layer, 50 wt.% NiCrAlY + 50 wt.% $ZrO_2$; *d* — internal NiCrAlY layer (*b*–*d* — ×500)

(see Table 4). In contrast to the initial powders, two new phases β-NiAl and NiO, as well as α-Cr, formed as a result of thermal and physical-chemical interaction of the spraying material with the plasma jet.

Structure, phase composition and microhardness of intermediate cermet layers of the three- (Figure 4) and five-layer (Figure 5) coatings almost coincided with corresponding characteristics of the coatings from mechanical mixtures of the same composition (see Figure 3, Table 4). Evaluation of the degree of tetragonality of the protective layer of the three- and five-layer coatings showed that it was 1.0103 and 1.0108, respectively. Therefore, in this case the tetragonal phase was also close to the T′-$ZrO_2$ quench phase.

When tested to heat resistance, the samples with the two- and five-layer coatings (Table 5) withstood 1500 thermal cycles, exhibiting no external changes. The traces of fracture on the surfaces of both two- and multilayer coatings formed not earlier than after 2000 thermal cycles.

Microhardness of the two-layer $ZrO_2$–NiCrAlY coating (with total thickness of about 570 μm), having a lamellar structure of the nickel interlayer and a layer of $ZrO_2$ formed from the round particles (Figure 6, *a*), hardly changed (see Table 5, variant 1) compared with the initial state (see Table 2). After 2000 thermal cycles of the tests, a longitudinal crack propagating into the $ZrO_2$ layer initiated within the zone of interface with the interlayer. Moreover, the surface layer of the $ZrO_2$ coating exhibited a negligible fracture (Figure 6, *b*). Only two phases, i.e. the tetragonal $ZrO_2$ phase (dominant) and an insignificant amount of the monoclinic $ZrO_2$ phase (about 1 wt.%), were fixed in the X-ray pattern, this corresponding to phase composition of the surface layer of the coating before the tests (see Table 2).

Multilayer coatings of the $ZrO_2$–NiCrAlY system, approximately 500 μm thick, had no cracks, delaminations and exfoliations from the substrate after the tests. However, the surface ceramic layer exhibited a heavy fracture (Figure 6, *c, d*). The X-ray pattern in Figure 7 shows, in addition to the two zirconia phases (tetragonal and monoclinic), also the presence of phases γ′-$Ni_3Al$ and β-NiAl, oxides NiO, as well as α-$Al_2O_3$, which is a product of oxidation of NiCrAlY, this being indicative of violation of integrity of the external layer after 2000 thermal cycles. Microhardness of the multilayer coating, which grew in the initial sample with increase in the content of the ce-

**Table 4.** Characteristics of plasma coatings produced from NiCrAlY and $ZrO_2$ powders and their mixtures

| Powder composition, wt.% | Coating thickness, μm | Phase composition | *HV*, MPa |
|---|---|---|---|
| 100NiCrAlY | 90 ± 15 | γ-Ni, γ′-$Ni_3Al$, β-NiAl, α-Cr | 3110 ± 560 |
| 25$ZrO_2$ + 75NiCrAlY | 100 ± 20 | γ-Ni, T-$ZrO_2$, γ′-$Ni_3Al$, β-NiAl, NiO, α-Cr, M-$ZrO_2$ | 4760 ± 1810 |
| 50$ZrO_2$ + 50NiCrAlY | 90 ± 20 | γ-Ni, T-$ZrO_2$, γ′-$Ni_3Al$, β-NiAl, NiO, M-$ZrO_2$, α-Cr | 5150 ± 1190 |
| 75$ZrO_2$ + 25NiCrAlY | 100 ± 20 | T-$ZrO_2$, γ-Ni, γ′-$Ni_3Al$, β-NiAl, NiO, M-$ZrO_2$, α-Cr | 7310 ± 2250 |
| 100$ZrO_2$ | 200 ± 20 | T-$ZrO_2$, M-$ZrO_2$ (traces) | 11,450 ± 1350 |

**Table 5.** Characteristics of TBC after heat resistance tests*

| Variant No. | Composition of spraying powder (layer-by-layer), wt.% | Thickness of layers, μm | *HV*, MPa | Fracture region |
|---|---|---|---|---|
| 1 | 100NiCrAlY | 120 | 2950 ± 500 | Longitudinal crack in $ZrO_2$ layer within the interlayer interface zone |
| | $100ZrO_2$ | 450 | 11,000 ± 1200 | |
| 2 | 100NiCrAlY | 100 | 2820 ± 560 | Fracture to 75 % of $ZrO_2$ layer; underlying layers are crack- and exfoliation-free |
| | $25ZrO_2$ + 75NiCrAlY | 80 | 4630 ± 590 | |
| | $50ZrO_2$ + 50NiCrAlY | 120 | 5030 ± 860 | |
| | $75ZrO_2$ + 25NiCrAlY | 100 | 6850 ± 1000 | |
| | 100 $ZrO_2$ | 100 | 9560 ± 1100 | |

*Quantity of thermal cycles to fracture was 2000.

ramic component from the interlayer to the $ZrO_2$ layer (see Table 4), hardly changed in value (see Table 5, variant 2).

A thermocouple was calked on the opposite side of a sample to a depth of 2 mm to reveal dynamics of heating of the coatings. It fixed growth of temperature of the uncoated substrate, as well as of the two- and five-layer coatings. Up to 10 heating and cooling cycles were carried out. Analysis of cyclograms of the samples showed that maximal heating temperature of the samples with TBC decreased from 415 (without coating) to 365 and 345 °C (for two- and five-layer coatings, respectively).

Therefore, phase composition of the external ceramic layer (content of the monoclinic $ZrO_2$ phase and tetragonal T′-phase with a low degree of tetragonality) depends upon the thickness of the metallic interlayer. Thickness of the metallic interlayer

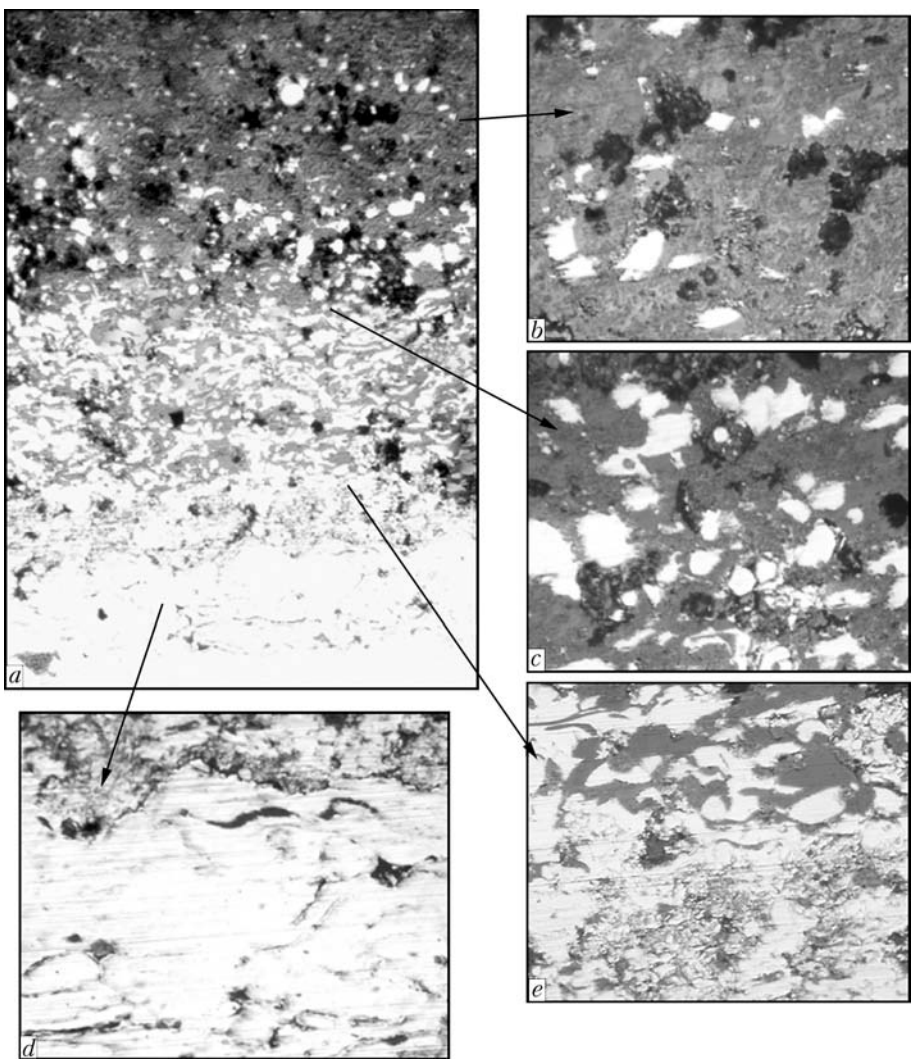


**Figure 5.** Microstructure of five-layer plasma coating: *a* — general view (×100); *b* — layer 75 wt.% $ZrO_2$ + 25 wt.% NiCrAlY; *c* — 50 wt.% $ZrO_2$ + 50 wt.% NiCrAlY; *d* — 25 wt.% $ZrO_2$ + 75 wt.% NiCrAlY; *e* — NiCrAlY (*b*–*e* — ×500)

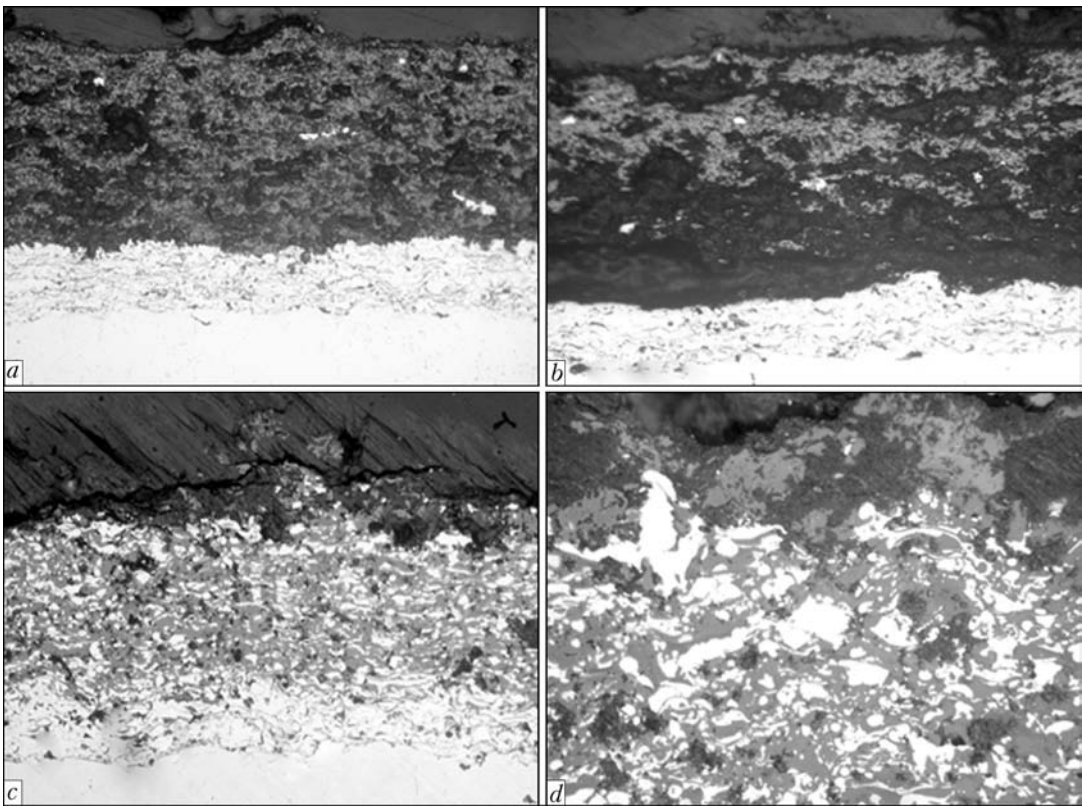


**Figure 6.** Microstructure of two- (×200) (*a, b* — see the text) and five-layer (*c* — ×100; *d* — ×400) coatings $ZrO_2$–NiCrAlY after heat resistance tests

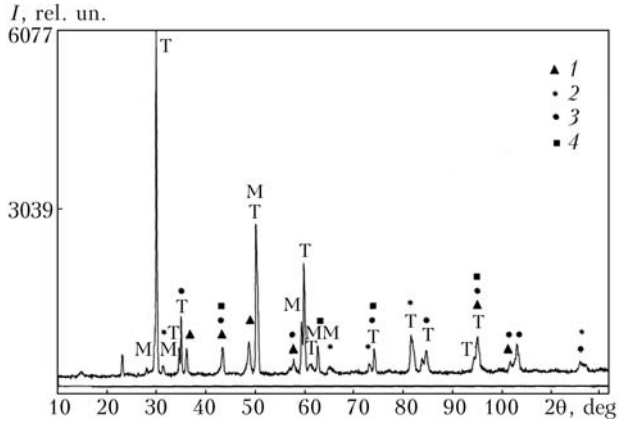


**Figure 7.** X-ray pattern of multilayer $ZrO_2$–NiCrAlY coating after heat resistance tests: *1* — γ′-$Ni_3Al$; *2* — β-NiAl; *3* — α-$Al_2O_3$; *4* — NiO

should not exceed 100 μm to provide the optimal phase composition of the ceramic layer, i.e. the monoclinic phase content of no more than 4 wt.% and maximal content of the T′-phase, which is responsible for heat resistance under thermal cycling conditions.

It was established as a result of investigation of three- and five-layer coatings produced by using heat-resistant alloy–ceramics mechanical mixtures that their phase composition, microhardness and structure gradually changed in a direction from the substrate to external ceramic layer. Metallographic analysis revealed no cracks, exfoliations from the substrate and delaminations in the coatings.

The thermal barrier coatings withstood not less than 2000 thermal cycles in investigation of heat resistance of the two- and five-layer metal–ceramic coatings under thermal cycling conditions (heating with a gas flame jet to 400 °C for 3 s with subsequent cooling to 20 °C). Analysis of cyclograms of samples with the two- and five-layer coatings showed that these coatings allow decreasing temperature of the aluminium substrate by 50 and 70 °C, respectively.

1. Nikitin, M.D., Kuliya, A.Ya., Zakharov, N.I. (1977) *Thermal-barrier and wear-resistant coatings on engine parts*. Leningrad: Mashinostroenie.
2. Iliushenko, A.F., Okovity, V.A., Kundas, S.P. et al. (2002) *Formation of thermal coatings: theory and practice*. Ed. by A.F. Iliushenko. Minsk: NIIPMeOP.
3. Iliushenko, A.F., Ivashko, V.S., Okovity, V.A. et al. (1998) *Thermal-barrier $ZrO_2$-base coatings*. Minsk: NIIPMeOP.
4. Rutman, D.S., Toropov, Yu.S., Pliner, S.Yu. et al. (1985) *High-refractory zirconia materials*. Moscow: Metallurgiya.
5. Pliner, S.Yu., Dabizha, A.A. (1987) Hardening of zirconia ceramics through tetragonal-monoclinic transformations. *Ogneupory*, **3**, 58–62.
6. Khor, K.A., Gu, Y.W. (1997) Plasma spraying of functionally graded NiCrAlY/yttria stabilized zirconia coating using pre-alloyed powders. In: *Proc. of United Forum for Sci. and Technol. Advances on Thermal Spray* (Ohio, USA). Ohio: ASM Int., Materials Park, 259–265.
7. (1995) *Superalloys: Heat-resistant materials for aerospace and industrial power units*. Ed. by Ch.T. Sims, N.S. Stoloff, U.K. Hagel. Book 2. Ed. by R.E. Shalin. Moscow: Metallurgiya.
8. Frolov, Z.A., Poklad, V.A., Ryabenko, B.V. et al. (2004) Technological peculiarities of deposition of thermal-barrier coatings in production of gas turbine blades. *Svarochn. Proizvodstvo*, **11**, 39–41.
9. Kolomytsev, P.T. (1991) *High-temperature protective coatings for nickel alloys*. Moscow: Metallurgiya.